GSA Data Repository 2015354

Cold-based Laurentide ice covered New England's highest summits during the Last Glacial Maximum

Supplemental Information – Bierman et al.

1. Laboratory and data reduction methods

For ^{10}Be and ^{26}Al analysis, about 250 µg of 1000 ppm SPEX ^{9}Be carrier was added to each sample and to the two process blanks included with each batch of 6 samples. If needed, ^{27}Al carrier was added to samples and about 2000 µg of ^{27}Al (1000 ppm SPEX Al standard) was added to the process blanks. We removed two small aliquots (representing 2.5% and 5% of the sample, respectively) from each sample directly following digestion. Using these aliquots, the total mass of Al and Be was quantified using Inductively Coupled Plasma Optical Emission Spectrometry. Following isolation of Be and Al, samples were oxidized, mixed with Ag powder, and packed into cathodes for isotopic analyses at Lawrence Livermore National Laboratory.

When measured, Al data were normalized to standard KNSTD9919 with an assumed ^{26}Al/^{27}Al ratio of 9919 x10^{-15}. When measured, Be data were normalized to standards LLNL1000 and LLNL3000 with assumed ^{10}Be/^{9}Be ratios of 1000 and 3000 x 10^{-15} (see Table DR2). Median ratios (and one standard deviation) for blanks processed with samples from New England were 2.40±1.81 x 10^{-15} for ^{26}Al/^{27}Al (n=8) and 2.44±0.23 x 10^{-14} for ^{10}Be/^{9}Be (n=9). These ratios were subtracted from measured ratios and the uncertainty propagated in quadrature.

Approximately 5 g of pure quartz from two of the samples (PTK-07 and PTMW-3) was processed for *in situ* ^{14}C analysis following Lifton et al. (2001) and Miller et al. (2006) using extraction and purification systems at the University of Arizona. *In situ* ^{14}C was extracted from each sample using the recirculating system and techniques described by Lifton et al. (2001), Pigati et al. (2010), and Miller et al. (2006). The ^{14}C content of the samples was analyzed at the Arizona AMS Laboratory and blank-corrected following Lifton et al. (2001), using data reduction techniques described by Hippe and Lifton (2014).

Exposure ages (^{10}Be and ^{26}Al) were calculated using the CRONUS calculator (wrapper script: 2.2, main calculator: 2.1, constants: 2.2.1, muons: 1.1, Balco et al., 2008), assuming the northeastern North American production rate and Lal (1991)/Stone (2000) time invariant scaling (Balco et al., 2008) using the standards against which the samples were measured and the concentrations calculated from the measured isotopic ratios, the mass of quartz used, and the amount of stable ^{27}Al and ^{9}Be present (see Table DR2). Note that the concentrations in Table 2 reflect the assumed value of standards at the time of measurement and that use of the CRONUS calculator takes into account recent changes in nominal values for these standards. The ^{26}Al/^{10}Be ratios in Table DR1 correspond to those generated using the standard values now generally accepted (Nishiizumi et al., 2007).

In situ ^{14}C ages were calculated using a version of the CRONUS calculator (available from http://hess.ess.washington.edu/math/al_be_v22/functionlist.html modified for use with *in situ* ^{14}C and Lal (1991)/Stone (2000) time invariant scaling. Global production rates for *in situ* ^{14}C were derived using calibration datasets from Lake Bonneville, Utah (Lifton et al., 2015), northwestern Scotland (Dugan, 2008), New Zealand (Schimmelpfennig et al., 2012), and western Greenland (Young et al., 2014). Each dataset was first recalculated following Hippe and Lifton (2014). Replicate analyses on individual samples were combined using inverse relative error-weighted means, and each site was then calibrated to a sea level, high latitude (SLHL) production rate

separately using CRONUS calculator code. The arithmetic mean and standard deviation of the site-derived SLHL production rates was then computed and used in the exposure age calculations. Note that the lack of regional ^{14}C calibration data means that we must rely on a global calibration.

2. Additional calculations: snow and ice cover, burial effect on $^{26}Al/^{10}Be$ ratio

It is possible that seasonal snow or ice cover could have reduced exposure ages. For example, reducing an exposure age from 14.5 to 12 ky requires a nearly 20% reduction in cosmic ray dosing, which could be achieved by covering the samples with ~35 cm of water equivalent year-round (Schildgen et al., 2005). Since soft rime and wet snow, both common on the summits, have densities ranging between 0.2 and 0.6 g cm^{-3} (COST-727, 2007), to achieve the reduction in age that we measure there would need to be between 1 and 3 m of frozen material present for 6 months per year since deglaciation 15 ky. This amount seems to be more ice and snow than is present today.

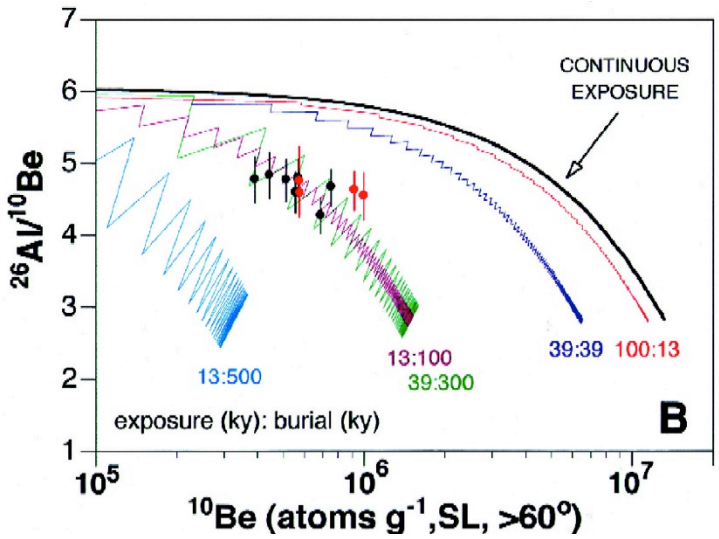

Figure DR1. Diagram from Bierman et al. (1999) showing trajectories of samples exposed and buried. When exposure exceeds burial or is equal to burial in duration, it takes many glacial/interglacial cycles before the $^{26}Al/^{10}Be$ ratio diverges enough from the production ratio that such changes are detectable.

Intermittent burial of sampled outcrops by ice has minimal effect on the $^{26}Al/^{10}Be$ ratio of subsequently exposed rocks when exposure duration is greater than or equal to burial duration. As shown by Bierman et al. (1999), only samples that have on average been buried for many times longer than they have been exposed will have $^{26}Al/^{10}Be$ ratios that are reliably below those resulting from steady exposure at the surface. In the case here, we posit <30 ky of burial by ice and 90 ky of exposure. As shown by the plot below (from Bierman et al., 1999) even a 50:50 ratio of burial to exposure would alter the ratio so that it dropped detectably below the steady exposure line only after many exposure/burial cycles with no surface erosion. Similar results are reported by Fabel and Harbor (1999).

Table DR1. Sample location and age data, New England summits

Sample	Site Location and Description	Elevation (m)	Latitude	Longitude	Thickness (cm)	^{26}Al Age (yr)*	^{10}Be Age (yr)*	Uncertainty-weighted average exposure age (yr)	^{26}Al/^{10}Be Ratio@	^{14}C Age (yr)#
PTD94-19	Franconia Ridge: ~200 m north of Little Haystack summit, glacially molded bedrock	1575	44.14078	-71.64402	3.0	59860 ± 3210	59390 ± 3310	59630 ± 2300	6.74 ± 0.23	
PTD94-20	Mount Washington: "Goofer Point," ~100 m SW of summit, glacially molded bedrock	1896	44.26982	-71.30483	3.0	18010 ± 1600	18570 ± 1010	18410 ± 850	6.54 ± 0.51	
PTD94-21	Mount Washington: "Goofer Point," ~100 m SW of summit, glacially molded bedrock	1896	44.27004	-71.30483	3.0	18200 ± 1030	17650 ± 950	17900 ± 700	6.96 ± 0.26	
PTMW-01	Mount Washington: "Goofer Point," ~100 m SW of summit, glacially molded bedrock	1896	44.27049	-71.30483	1.0	25370 ± 1730	27790 ± 1500	26750 ± 1130	6.15 ± 0.33	
PTMW-02	Mount Washington: "Goofer Point," ~100 m SW of summit, glacially molded bedrock	1896	44.27049	-71.30483	3.0	73910 ± 4140	69350 ± 3650	71340 ± 2740	7.09 ± 0.22	
PTMW-03	Mount Washington: summit, ~20 m N of Tip Top House, frost-riven block, perched atop larger frost-riven block	1895	44.27049	-71.30483	2.0	149200 ± 8200	156100 ± 8330	152600 ± 5840	6.26 ± 0.16	12710 ± 2770
PTMW-04	Mount Washington: Tuckerman Ravine, landslide block that was reoriented by a late-glacial rock glacier	1326	44.26149	-71.29511	1.0	12590 ± 1140	12590 ± 700	12590 ± 600	6.76 ± 0.55	
PTK-06	Baxter Peak, Katahdin Summit, glacially molded bedrock	1606	45.90422	-68.92161	4.0	9280 ± 600	9860 ± 540	9600 ± 400	6.36 ± 0.32	
PTK-07	Baxter Peak, Katahdin Summit, angular block perched atop bedrock with sample PTK-06	1607	45.90471	-68.92191	4.0	37260 ± 2070	34310 ± 1770	35560 ± 1350	7.29 ± 0.23	11040 ± 2190

*Ages calculated from Lal (1991)/Stone (2000) scaling scheme using CRONUS (Balco et al., 2008) assuming no geomagnetic correction and assuming northeastern North American production rate (Balco et al., 2009). Uncertainty is external error from CRONUS (Balco et al., 2008). CRONUS considers different standards used to normalize isotope ratio measurements. Topographic sheilding was negligable for all samples.

#Assuming production rate of 12.7 ± 1.1 atoms/(g*yr) and Lal/Stone scaling scheme

@^{26}Al/^{10}Be ratio calculated by CRONUS and normalized to accepted value of AMS standards per Nishiizumi et al. (2007)

Coordinates in WGS84

all uncertainties are 1 standard deviation
Lithologies are as follows :Baxter Peak, Katahdin, Granophyric phase of Katahdin Granite pluton, coarse-grained beige or pink to red, porphyritic biotite-bearing granophyre with cavities and vugs; Little Haystack, Mount Lafayette unit of White Mountain batholith, medium-grained gray, red, or green granite porphyry with quartz phenocrysts; Mt. Washington, Huntington Ravine member of Littleton Formation, coarse-grained gray, thin, evenly bedded schist and quartzite, folded and refolded, with blebs and veins of quartz

Table DR2. Isotopic Measurements, New England Summits

Sample Name	Quartz Mass (g)	Be Carrier (g)*	Al Carrier (g)*	Measured Total Al (ug)**	Measured $^{10}Be/^{9}Be$ Ratio***	$^{10}Be/^{9}Be$ Ratio Unc.	Measured $^{26}Al/^{27}Al$ Ratio***	$^{26}Al/^{27}Al$ Ratio Unc.	^{10}Be Conc. (atoms g^{-1}) ****	^{10}Be Unc. (atoms g^{-1})	^{26}Al Conc. (atoms g^{-1}) ****	^{26}Al Unc. (atoms g^{-1})
PTD94-19	39.230	0.252	0.000	7579	2.303E-12	6.049E-14	1.321E-12	2.674E-14	9.782E+05	2.599E+04	5.696E+06	1.154E+05
PTD94-20	25.360	0.253	0.000	27732	6.139E-13	1.439E-14	9.134E-14	6.745E-15	3.933E+05	9.717E+03	2.224E+06	1.647E+05
PTD94-21	41.320	0.251	0.000	7724	9.452E-13	2.187E-14	5.396E-13	1.566E-14	3.739E+05	8.929E+03	2.248E+06	6.541E+04
PTMW-01	26.650	0.254	0.000	15620	9.611E-13	2.256E-14	2.431E-13	1.141E-14	5.969E+05	1.444E+04	3.175E+06	1.493E+05
PTMW-02	30.890	0.355	0.000	29769	1.905E-12	3.652E-14	4.132E-13	1.019E-14	1.450E+06	2.808E+04	8.884E+06	2.193E+05
PTMW-03	39.409	0.253	0.576	3229	7.524E-12	1.372E-13	9.528E-12	1.661E-13	3.218E+06	5.888E+04	1.742E+07	3.039E+05
PTMW-04	40.228	0.355	0.000	20341	3.168E-13	7.961E-15	9.184E-14	6.976E-15	1.767E+05	4.796E+03	1.033E+06	7.878E+04
PTK-06	39.915	0.254	0.000	7106	4.330E-13	1.017E-14	2.416E-13	1.034E-14	1.739E+05	4.438E+03	9.565E+05	4.118E+04
PTK-07	40.730	0.254	0.000	7060	1.364E-12	2.317E-14	9.809E-13	2.541E-14	5.584E+05	9.706E+03	3.792E+06	9.835E+04

*Be and Al carriers added to samples both had a concentration of 1000 ppm.

**Refers to the total Al in the sample (including both native Al in quartz and Al added via carrier, if applicable) quantified in duplicate by ICP-OES directly following digestion.

***During AMS analysis, all Be samples were normalized to standard LLNL3000 (except sample PTK-07, which was normalized to LLNL 1000) and all Al samples were normalized to standard KNSTD9919.

****Concentration considering accepted value of standards at time of measurement, late 1990s, used for CRONUS

all uncertainties are one standard deviation

Table DR3: In situ ^{14}C sample analytical data

Sample Name	Lab Number	AMS Number	Mass Quartz *(g)*	V_{CO2} *(mL)*	V_{dil} *(mL)*	F_M	$[^{14}C]$ 10^5 *at* g^{-1}
PTK-07	RN-785	AA-54556	4.9975	0.0137 ± 0.0011	2.1115 ± 0.0203	0.0271 ± 0.0006	3.3534 ± 0.1130
PTMW-03	RN-786	AA-54557	5.0069	0.0443 ± 0.001	1.3774 ± 0.0131	0.0527 ± 0.0007	4.3015 ± 0.1036

Notes: $\delta^{13}C$ of both diluted samples assumed to be -35.0 ± 2.0 ‰ (typical value for diluted samples). Uncertainty in quartz mass: ±0.0002 g. Fraction modern (F_M) values corrected per Hippe and Lifton (2014). Concentration calculated after subtracting long-term extraction system process blank of (1.2367 ± 0.3531) x 10^5 ^{14}C atoms.

Table DR4. Selected radiocarbon ages older than Last Glacial Maximum from New England

Site Name	Latitude (°N)	Longitude (°W)	^{14}C Age (yr BP)	Lab Number	Material	Calibrated Age (ka BP)[a]	Original Reference
Gould Pond	44 59 33	69 19 09	25280±1010	SI-5372	marine shells	29040 (27106-31083)	Anderson et al., 1992
Isie Lake	47 04 15	68 39 23	24300±110	OS-6435	paleosol	28340 (28020-28652)	Dorion, 1997
Jo Mary Pond	45 34 38	68 02 19	24500±130	OS-3170	paleosol	28550 (28208-28829)	Dorion, 1997
Upper South Branch Pond	46 05 00	68 54 00	29200±550	SI-4519	wood	33240 (31763-34275)	Anderson et al., 1986

[a]Age estimates include the median intercept and the minimum and maximum ages in parentheses based on 2 standard deviations from minimum and maximum intercepts using CALIB 7.0 (Reimer et al., 2014) and considering combined IntCal04/Marine04

Note, original information compiled in Dorion, 1997

7. Maps of sampling sites

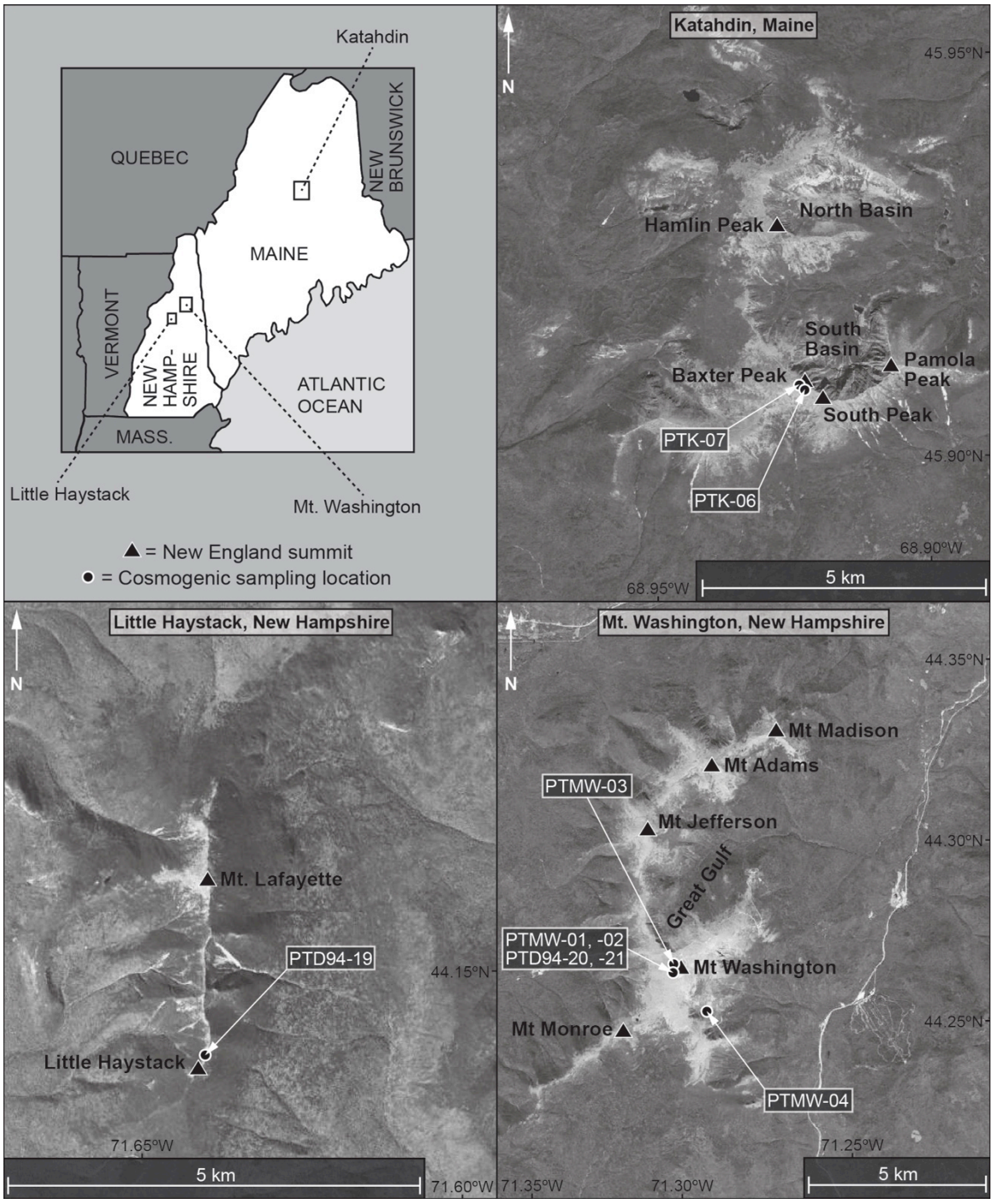

Figure DR2. Air photographs (base from Google Earth) showing location of samples used in this study. Map in upper left shows location of the three air photograph panels. Coordinates for each sample site provided in Table DR1.

8. Modeled ice profiles and explanation/approach

We used a simple spreadsheet model for ice profiles based on the model of Nye (1952) following the approach of Davis (1989). We presume that the ice margin extended to near Martha's Vineyard at the Last Glacial Maximum (LGM). To get Mt. Washington exposed at the LGM requires a basal shear stress <0.5 bar, which is unlikely on the bare crystalline rock terrain in the uplands of New England. Basal shear stresses >0.5 bar bury the summit in ice. Having thin ice over the peaks is likely important not only to keep the ice cold but to prevent pressure melting and glacial erosion. We conclude that basal shear stress in the rough, mountainous terrain of central New England was at least 0.5 bars.

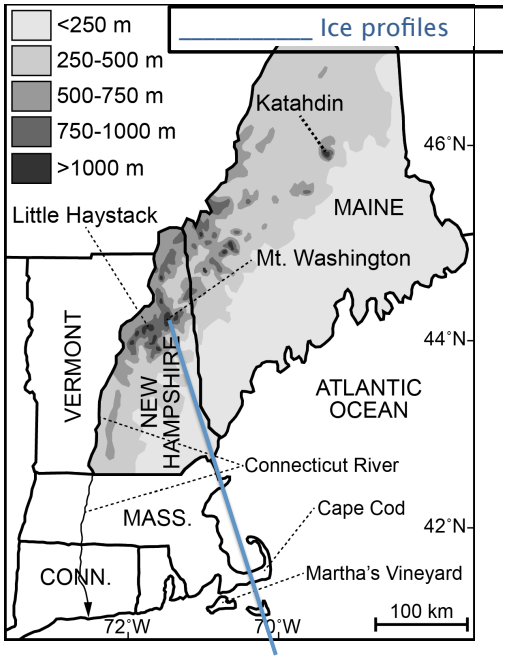

Figure DR3

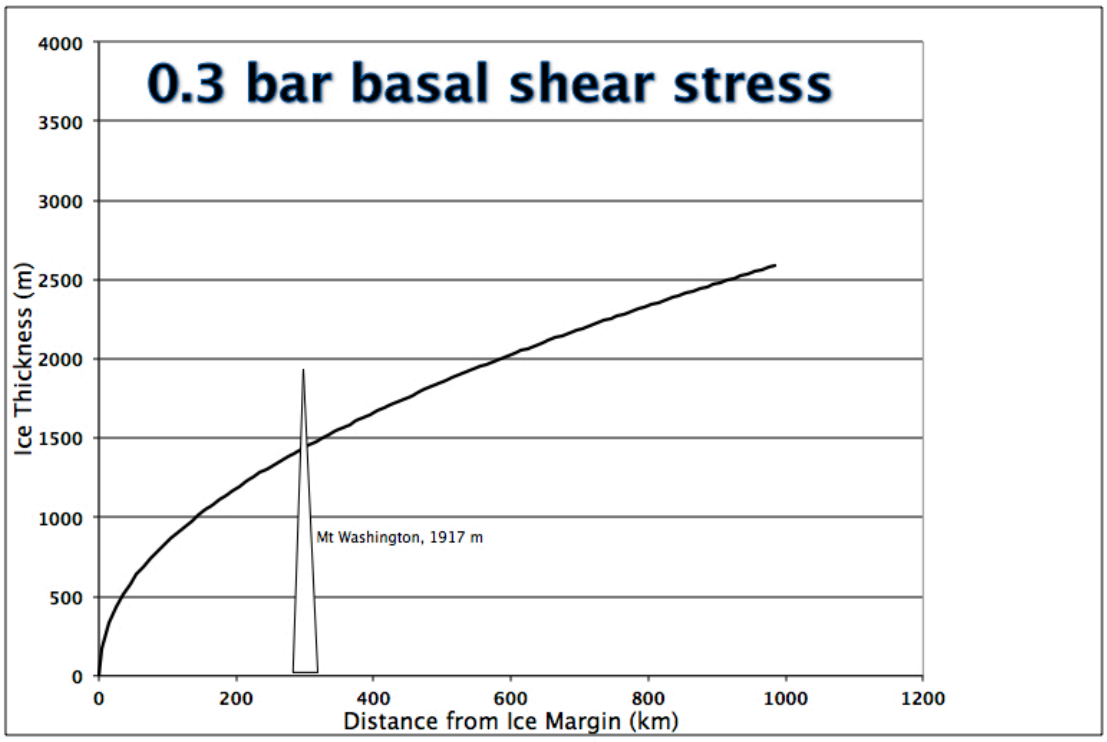

Figure DR4. Ice sheet profile model based on the equation of Nye (1952) for basal shear stress = 0.3 bar at Last Glacial Maximum. Summit is exposed, which is not consistent with isotopic data.

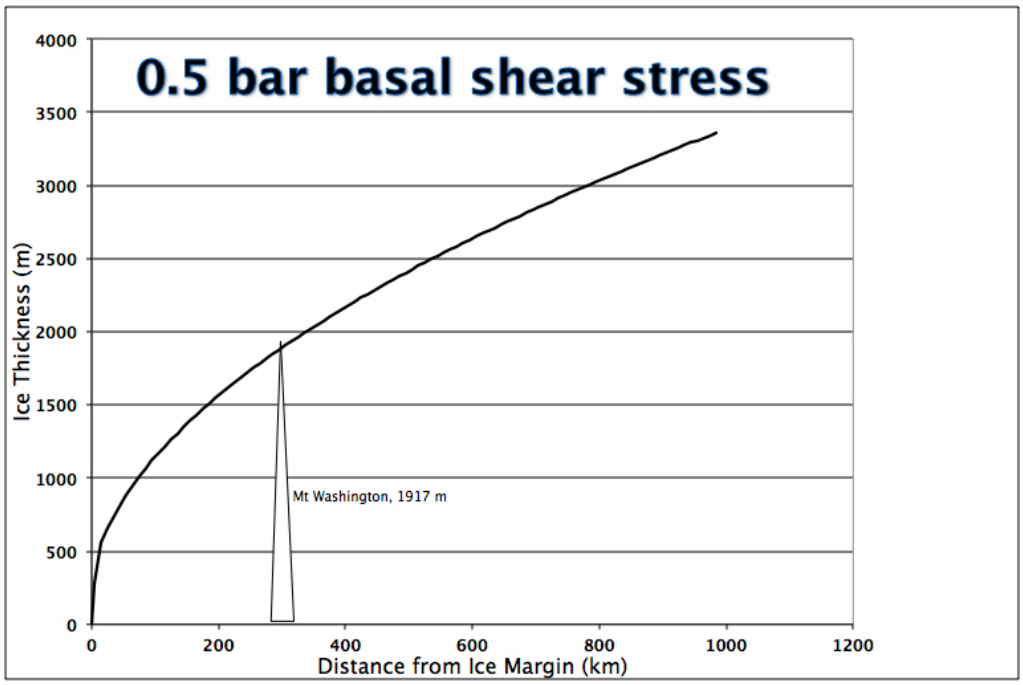

Figure DR5. Ice sheet profile model based on the equation of Nye (1952) for basal shear stress = 0.5 bar at Last Glacial Maximum. Summit is just covered by ice. This model is most consistent with isotopic data indicating cold-based ice at the summit and erosive, warm-based ice just below.

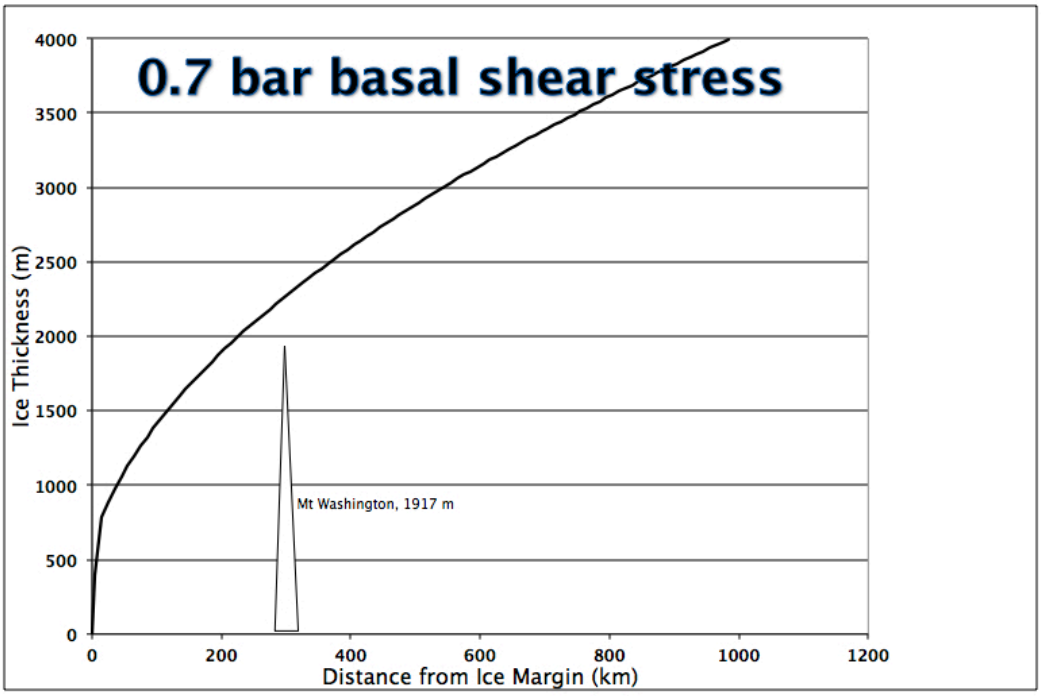

Figure DR6. Ice sheet profile model based on the equation of Nye (1952) for basal shear stress = 0.7 bar at Last Glacial Maximum. Summit is deeply buried by ice that is likely warm based and not consistent with isotopic data.

9. References Cited in Supplemental Information

Anderson, R.S., Davis, R.B., Miller, N.G., and Stuckenrath, R. 1986, History of late- and post-glacial vegetation and disturbance around Upper South Branch Pond, northern Maine: Canadian Journal of Botany, v. 64, p. 1977-1986.

Anderson, R.S., Jacobson, G.L., Jr., Davis, R.B., and Stuckenrath, R., 1992, Gould Pond, Maine: Late-glacial transitions from marine to upland environments: Boreas, v. 21, p. 359-371.

Balco, G., Stone, J.O., Lifton, N.A., and Dunai, T.J., 2008, A complete and easily accessible means of calculating surface exposure ages or erosion rates from ^{10}Be and ^{26}Al measurements: Quaternary Geochronology, v. 3, p. 174-195.

Balco, G., Briner, J., Finkel, R.C., Rayburn, J.A., Ridge, J.C., and Schaefer, J.M., 2009, Regional beryllium-10 production rate calibration for late-glacial northeastern North America: Quaternary Geochronology, v. 4, p. 93-107.

Bierman, P.R., Marsella, K.A., Patterson, C., Davis, P.T., and Caffee, M., 1999, Mid-Pleistocene cosmogenic minimum-age limits for pre-Wisconsinan glacial surfaces in southwestern Minnesota and southern Baffin Island; a multiple nuclide approach: Geomorphology, v. 27, no. 1-2, p. 25-39.

COST-727, Atmospheric Icing on Structures: 2007, Measurements and data collection on icing: State of the Art, MeteoSwiss, 75, 110 pp.

Davis, P.T., 1989. Late Quaternary glacial history of Mt. Katahdin and the nunatak hypothesis. In: Tucker, R.D. and Marvinney, R.G. (Editors), Studies in Maine Geology, Quaternary Geology. Maine Geological Survey, Augusta, pp. 119-134.

Dorion, C.C., 1997, An updated high resolution chronology of deglaciation and accompanying marine transgression in Maine [M.S. thesis]: Orono, University of Maine, 147 p.

Dugan, B., 2008, New production rate estimates for in situ cosmogenic ^{14}C from Lake Bonneville, Utah, and Northwestern Scotland [M.S. thesis]: University of Arizona, Geosciences Department, 46 p.

Fabel, D. and Harbor, J., 1999, The use of in-situ produced cosmogenic radionuclides in glaciology and glacial geomorphology: Annals of Glaciology, v. 28, p. 103-110.

Hippe, K., and Lifton, N.A., 2014, Calculating isotope ratios and nuclide concentrations for in situ cosmogenic ^{14}C analyses: Radiocarbon, v. 56, no. 3, p. 1167-1174.

Lal, D., 1991, Cosmic ray labeling of erosion surfaces; in situ nuclide production rates and erosion models: Earth and Planetary Science Letters, v. 104, no. 2-4, p. 424-439.

Lifton, N., Jull, A., and Quade, J., 2001, A new extraction technique and production rate estimate for in situ cosmogenic ^{14}C in quartz: Geochimica Et Cosmochimica Acta, v. 65, p. 1953-1969.

Lifton, N., Caffee, M., Finkel, R., Marrero, S., Nishiizumi, K., Phillips, F.M., Goehring, B., Gosse, J., Stone, J., Schaefer, J., Theriault, B., Jull, A.J.T., and Fifield, K., 2015, In situ cosmogenic nuclide production rate calibration for the CRONUS-Earth project from Lake Bonneville, Utah, shoreline features: Quaternary Geochronology, v. 26, p. 56-69.

Miller, G., Briner, J., Lifton, N., and Finkel, R.C., 2006, Limited ice-sheet erosion and complex exposure histories derived from in situ cosmogenic ^{10}Be, ^{26}Al, and ^{14}C on Baffin Island, Arctic Canada: Quaternary Geochronology, v. 1, no. 1, p. 74-85.

Nishiizumi, K., Imamura, M., Caffee, M.W., Southon, J.R., Finkel, R.C. and McAninch, J., 2007. Absolute calibration of ^{10}Be AMS standards. Nuclear Inst. and Methods in Physics Research, B, v.258, n. 2, p. 403-413.

Nye, J.F., 1952, A method of calculating the thickness of the ice-sheets. Nature, v. 169 n. 4300, p. 529-530.

Pigati, J., Lifton, N., Jull, A., and Quade, J., 2010, A simplified in situ cosmogenic ^{14}C extraction system. Radiocarbon, v. 52, p. 1236-1243.

Reimer, P.J., Reimer, R., and Stuiver, M., 2014. CALIB 7.0 radiocarbon calibration program. http://calib.qub.ac.uk/calib/

Schildgen, T.F., Phillips, W.M., and Purves, R.S., 2005, Simulation of snow shielding corrections for cosmogenic nuclide surface exposure studies: Geomorphology, v. 64, no. 1-2, p. 67-85.

Schimmelpfennig, I., Schaefer, J.M., Goehring, B.M., Lifton, N., Putnam, A.E., and Barrell, D.J.A., 2012, Calibration of the in situ cosmogenic ^{14}C production rate in New Zealand's Southern Alps: Journal of Quaternary Science, v. 27, no. 7, p. 671-674.

Stone, J., 2000, Air pressure and cosmogenic isotope production: Journal of Geophysical Research, v. 105, no. b10, p. 23753-23759.

Young, N.E., Schaefer, J.M., Goehring, B., Lifton, N., Schimmelpfennig, I., and Briner, J.P., 2014, West Greenland and global in situ ^{14}C production-rate calibrations: Journal of Quaternary Science, v. 29, no. 5, p. 401-406.